

**DYNAMIC APERTURE PERFORMANCE FOR DIFFERENT
COLLISION OPTICS SCENARIOS FOR THE LHC LUMINOSITY
UPGRADE**

R. De Maria, S. Fartoukh, M. Giovannozzi, CERN, Geneva, Switzerland

A. Chancé, B. Dalena, J. Payet (CEA/IRFU, Gif-sur-Yvette),

J. Resta-López (IFIC, Valencia),

K. M. Hock, M. Korostelev, A. Wolski (The University of Liverpool, Liverpool)

Abstract

The ATS [1] optics solution for the HL-LHC offers the possibility of different collision optics, with a β^* as small as 10 cm in both transverse planes, or with a β^* aspect ratio of up to 4 pushing β^* to even smaller value (5 cm) in the parallel separation plane while relaxing it (20 cm) in the crossing plane. The latter configuration features two possible options for alternative orientations of the crossing plane in the two high luminosity insertions, both considered in this study. In this paper we study the impact of a few selected field imperfection models of the new magnets foreseen for the upgrade through tracking simulations and scaling laws.

Presented at the International Particle Accelerator Conference (IPAC'13) –

May 12-17, 2012, Shanghai, China

Geneva, Switzerland, May 2013



DYNAMIC APERTURE PERFORMANCE FOR DIFFERENT COLLISION OPTICS SCENARIOS FOR THE LHC LUMINOSITY UPGRADE*

R. De Maria, S. Fartoukh, M. Giovannozzi, CERN, Geneva, Switzerland
 A. Chancé, B. Dalena, J. Payet (CEA/IRFU, Gif-sur-Yvette),
 J. Resta-López (IFIC, Valencia),
 K. M. Hock, M. Korostelev, A. Wolski (The University of Liverpool, Liverpool)

Abstract

The ATS [1] optics solution for the HL-LHC offers the possibility of different collision optics, with a β^* as small as 10 cm in both transverse planes, or with a β^* aspect ratio of up to 4 pushing β^* to even smaller value (5 cm) in the parallel separation plane while relaxing it (20 cm) in the crossing plane. The latter configuration features two possible options for alternative orientations of the crossing plane in the two high luminosity insertions, both considered in this study. In this paper we study the impact of a few selected field imperfection models of the new magnets foreseen for the upgrade through tracking simulations and scaling laws.

OVERVIEW OF OPTICAL CONFIGURATIONS

The tracking studies have been carried out using the optics configurations developed in the SLHCV3.1b version of the HL-LHC layout [2].

The optics configurations of the high-luminosity insertions regions (IR) 1 and 5 are summarised in Table 1, which provides the values of β^* in the crossing and perpendicular planes, together with the values of the crossing angle, parallel separation (used prior to beam collisions) and the value of β_{\max} reached in the inner triplets (IT).

Table 1: Summary of the SLHCV3.1b optics configurations used for tracking studies presented in this paper. The values of β_{\max} refer to the peak β reached in the triplets.

	$\beta_{\times}^*/\beta_{\parallel}^*$ [m]	$\theta_{\times}/2$ [μrad]	\parallel sep/2 [mm]	β_{\max} [m]
injection	11.0/11.0	170	2	286
	5.5/5.5	245	2	539
pre-squeeze	2.0/2.0	80	2	1459
	0.40/0.40	180	0.75	7272
round	0.33/0.33	295	0.75	8815
	0.15/0.15	295	0.75	19393
	0.10/0.10	360	0.75	29090
flat	0.30/0.075	275	0.75	38786
	0.20/0.05	335	0.75	58180

* The HiLumi LHC Design Study is included in the HL-LHC project and is partly funded by the European Commission within the Framework Programme 7 Capacities Specific Programme, Grant Agreement 284404.

The first two options refer to possible configurations at injection energy, and possibly up to the end of the ramp. The injection optics with β^* of 5.5 m is introduced to profit from the increased aperture margins in the new IR magnets with respect to the nominal one with $\beta^* = 11$ m, which is also available.

All the other configurations refer to configurations at top energy. The pre-squeeze is the stage when β^* in IR1/5 is reduced without inducing the beta-beating wave in the neighbouring arcs, but when optimal ATS phasing conditions can be reached [1], while the remaining conditions represent squeeze optics with the full ATS scheme [1].

Both round beams at baseline and ultimate β^* of 15 cm and 10 cm, respectively, as well as flat beams at nominal and ultimate β^* of 7.5/30 cm and 5/20 cm are included in our study. In almost all cases the nominal orientation of the crossing angle is used, i.e., vertical in IR1 and horizontal in IR5. However, each flat beam optics has also an alternative crossing scheme with horizontal crossing in IR1 and vertical in IR5, always keeping the largest β^* in the crossing plane.

In the case of IR2 and IR8, the conditions are $\beta^* = 10$ m with an external half crossing angle of 170 μrad in vertical (IR2) and horizontal plane (IR8).

It is worth mentioning that while for the injection region the global β_{\max} refers to the location of Q5 in IR6, where β_v reaches 610 m, in all other optical configurations the global maximum value of the beta-functions occurs in the triplets and is equal to the value listed in Table 1.

SETTINGS FOR NUMERICAL SIMULATIONS

The various optical configurations have been probed to study the dependence of the dynamic aperture (DA) as a function of β^* and of the optics type (round or flat). The dynamic aperture has been computed over 10^5 turns, using a polar grid of initial conditions distributed in such a way to have 30 particles for each interval of 2σ . Furthermore, 59 values of the phase space angles have been used. The momentum offset has been set to 2.7×10^{-4} . The value of the normalised rms beam emittance is $\epsilon = 3.75 \mu\text{m}$ at 7 TeV.

As far as the magnetic imperfections are concerned, sixty realisations of the machine (also called seeds) have been used. The LHC ring has been simulated assigning the measured magnetic errors to all magnets (see, e.g., Ref. [3])

for an overview of similar studies for the nominal machine) apart from those magnets located in the high-luminosity insertions IR1 and 5. In these IRs only the new triplets have been assigned magnetic errors based on guess estimate of the proposed triplet's field quality [4]. The values used in the numerical simulations are reported in Table 2. It is

Table 2: Multipoles used for the field quality of the triplets. The values are in units of 10^{-4} at $R_{ref} = 50$ mm.

	Normal		Skew	
	Uncertainty (U)	Random (R)	Uncertainty (U)	Random (R)
3	0.712	0.712	0.712	0.712
4	0.512	0.512	0.512	0.512
5	0.368	0.368	0.368	0.368
6	1.440	1.440	0.264	0.264
7	0.168	0.168	0.168	0.168
8	0.128	0.128	0.128	0.128
9	0.064	0.064	0.064	0.064
10	0.048	0.048	0.048	0.048
11	0.032	0.032	0.032	0.032
12	0.021	0.021	0.021	0.021
13	0.014	0.014	0.014	0.014
14	0.009	0.009	0.009	0.009

worth recalling that in the framework of the LHC studies the magnetic errors have been split into three components, namely a mean (S), uncertainty (U), and random (R) such that a given multipole is obtained by

$$b_n = b_{n_S} + \frac{\xi_U}{1.5} b_{n_U} + \xi_R b_{n_R}, \quad (1)$$

where ξ_U, ξ_R are Gaussian distributed random variables cut at 1.5σ and 3σ , respectively. The ξ_U variable is the same for all magnets of a given class, but changes from seed to seed and for the different multipoles. On the other hand, ξ_R changes also from magnet to magnet. The values of $b_{n_S}, b_{n_U}, b_{n_R}$ are given in Table 2. Under these assumptions the field expansion for a dipole is given by

$$B_y + i B_x = B_{ref} \sum_{n=1}^N (b_n + i a_n) \left(\frac{x + i y}{R_{ref}} \right)^{n-1}. \quad (2)$$

Unlike other studies [5, 6], in this paper the assumed field quality for the new triplets has been considered as fixed and no scan over multipoles has been performed. Nevertheless, a second case in which all the coefficients reported in Table 2 as divided by two is also used for comparison.

It is also worth mentioning that in all numerical simulations reported in this paper the non-linear corrector package described in Ref. [7] has been used.

NUMERICAL RESULTS

The main outcome of the numerical simulations is shown in Fig. 1. In the upper plot the DA for several optical configurations with β^* below 100 cm is shown, while in the lower plot the DA for two special configurations at

$\beta^* = 200$ cm and 550 cm are also included. Not only round optics are included, but also flat optics with different crossing planes as mentioned in the first section. In addition, two sets of multipoles are included to assess the dependence of the DA on the overall field quality of the proposed triplets. The markers represent the average DA (over the seeds and

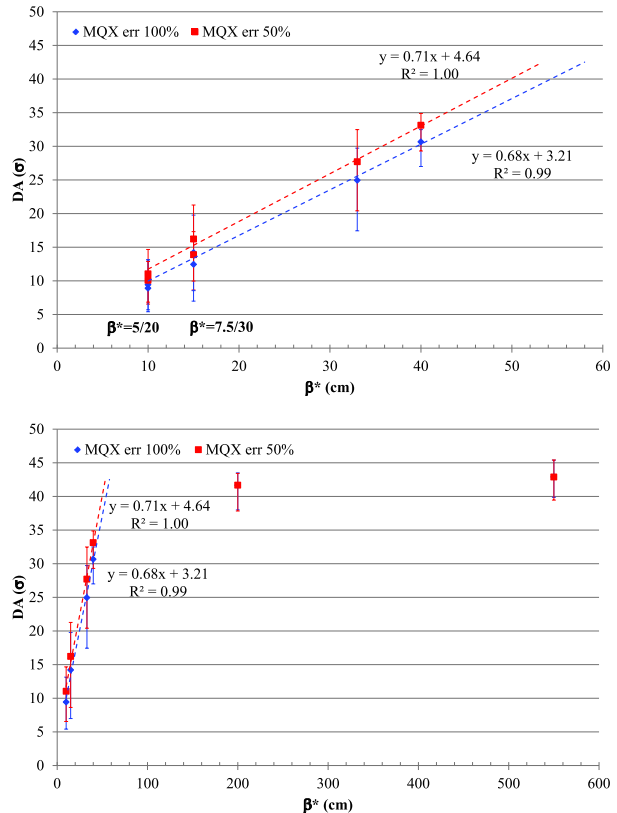


Figure 1: Dynamic aperture as a function of β^* below 100 cm (upper) and up to 550 cm (lower). Two situations are considered, corresponding to the field quality from Table 2 and to a factor of two better field quality. The linear behaviour of the DA is clearly seen for the round optics configurations.

the angles), while the negative error bars represent the minimum DA (over the seeds and the angles) and the positive error bars the average DA over the angles of the maximum over the seeds. In this way the spread introduced by the realisations and the phase space angles is made visible in a compact form.

In the case of the round optics the DA scales linearly with β^* . The slope of the straight line is the same, within the numerical errors on the fit parameters, for both sets of IT multipoles. On the other hand the constant term differs by about 1.5σ : this can be considered as the gain in terms of DA from a reduction by a factor of two in the multipoles of the ITs.

In the case of the flat beam optics, the corresponding DA values have been plotted associating them with the value of $\sqrt{\beta_x^* \beta_y^*}$. The DA is worse than the corresponding round optics by $1 - 2\sigma$. The slope is essentially the same as for the dependence of DA vs. β^* for the round optics, while the

constant term is smaller. In the case of the flat beam optics the improvement of the field quality of the triplets turns out to provide an increase in DA of 0.7σ , only. The fact that the DA dependence over β^* is not exactly the same for round and flat optics could be linked with the asymmetry in the optical configuration combined with the alternating crossing plane between IR1 and 5. Moreover, the DA does not show any dependence on the choice of the orientation of the crossing plane in the high-luminosity insertions.

In Fig. 2 the comparison between the shape of the DA for round (left) and flat (right) optics and different β^* values is shown. Apart from the reduction in surface area, the DA for flat optics looks like a square with a smaller size of the blue unstable area.

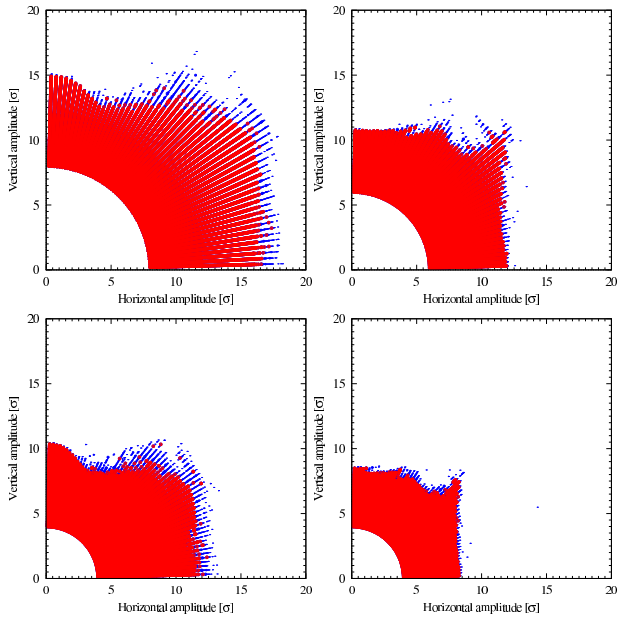


Figure 2: Dynamic aperture in normalised physical space for seed 1. The red area represents the region stable up to 10^5 turns; the blue one is the unstable region (the marker dimension is proportional to the stability of the initial condition); the white area around the origin represents stable particles that are not tracked. The situation for round and flat optics is represented in the left and right plots, respectively. Different β^* are represented, namely 15 and 10 cm in the upper and lower plots, respectively.

Above 200 cm of β^* the DA is almost constant as it can be seen in Fig. 1 (lower plot) and this value is determined by the machine elements other than the triplets in IR1 and 5. It is worth mentioning that, based on the linear fit, the constant DA value would be achieved for $\beta^* \approx 60$ cm. For these large values of β^* the beam dynamics is qualitatively different as it can be seen in Fig. 3.

Stable regions disconnected from the phase space region around the origin are clearly visible and non-negligible blue regions are present, indicating large areas where chaotic and unstable motion occur. Furthermore, the border does not feature any special symmetry between the horizontal and vertical planes, the DA being larger towards

higher angles in physical space, as at injection where DA is dominated by the field imperfections of the main dipoles.

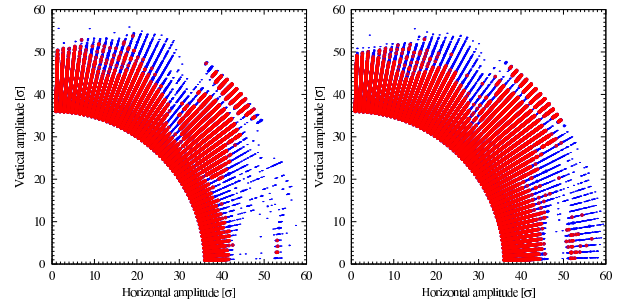


Figure 3: Dynamic aperture in normalised physical space for seed 1. The red area represents the region stable up to 10^5 turns; the blue one is the unstable region (the marker dimension is proportional to the stability of the initial condition); the white area around the origin represents stable particles that are not tracked. Only round optics configurations are shown for $\beta^* = 200$ cm (left) and 550 cm (right).

CONCLUSIONS

The results of detailed numerical simulations aimed at assessing the dependence of DA on the optical configuration have been presented in this paper. A linear dependence on β^* has been found for the round optics configurations. Flat optics options have been explored as well, but not enough to derive a scaling law on β^* . Nevertheless, if the DA of flat optics are compared with that of round optics with the same geometrical averaged β^* , then a small degradation is found.

The dependence on the field quality of the new triplets has been explored too, by considering two cases in which the nominal field quality or a re-scaled one by a factor of two is used. A gain of about 1.5σ for a reduction of a factor two in the field quality is obtained.

REFERENCES

- [1] S. Fartoukh, “An Achromatic Telescopic Squeezing (ATS) Scheme for LHC Upgrade”, WEPC037, Proc. IPAC11, p. 2088.
- [2] S. Fartoukh, R. De Maria, “Optics and Layout Solutions for HL-LHC with Large Aperture Nb3Sn and Nb-Ti Inner Triplets”, MOPPC011, Proc. IPAC12, p. 145.
- [3] S. Fartoukh, M. Giovannozzi, Nucl. Instrum. & Methods A **671**, p. 10, 2012.
- [4] E. Todesco, private communication, November 2012.
- [5] Y. Nosochkov *et al.*, “Optimization of Triplet Quadrupoles Field Quality for the LHC High Luminosity Lattice at Collision Energy”, TUPFI016, these proceedings.
- [6] Y. Nosochkov *et al.*, “Specification of Field Quality for Separation Dipoles and Matching Section Quadrupoles for the LHC High Luminosity Lattice at Collision Energy”, TUPFI017, these proceedings.
- [7] M. Giovannozzi, S. Fartoukh, R. De Maria, “Specification of a System of Correctors for the Triplets and Separation Dipoles of the LHC Upgrade”, WEPEA048, these proceedings.